

Research Article

Investigating the Influence of Zr⁴⁺ Content on the Crystal Structure, Micromorphology, Dielectric Properties of Ba(Zr_xTi_{1-x})O₃ Ceramics

Anant Kunwar

O.P Jindal University, Raigarh, Chattishgarh.

I N F O

E-mail Id:

anantkunwar75@gmail.com

orcid Id:

<https://orcid.org/0009-0009-7272-3113>

How to cite this article:

Kumar A. Investigating the Influence of Zr⁴⁺ Content on the Crystal Structure, Micromorphology, Dielectric Properties of Ba(Zr_xTi_{1-x})O₃ Ceramics. *J Adv Res Mfg Mater Sci Met Engi* 2023; 10(1): 15-20.

Date of Submission: 2023-03-05

Date of Acceptance: 2023-04-15

A B S T R A C T

By using a solid-state reaction technique, Ba(Zr_xTi_{1-x})O₃ ceramics (X=1.5, 2.0, 2.5, 3.0) were created. Controlling the Zr/Ti ratio has an impact on the dielectric characteristics, micromorphology, crystal structure of BZT ceramics. X-ray diffraction, scanning electron microscopy, impedance analysis were each used to characterise the crystal structures, morphologies, electric characteristics of the samples. The zirconium titanate ceramic samples exhibit cubic phase behaviour and no secondary phase, according to the X-ray diffraction patterns. The microstructure, dielectric characteristics, crystal structure are all significantly influenced by the Zr/Ti ratio. The lattice constant rises and the grain size falls as the Zr⁴⁺ content does. When the Zr content reaches 15%, the dielectric constant is at its highest. The dielectric constant steadily falls as the Zr⁴⁺ content rises, the Curie temperature gradually descends into the low temperature zone.

Keywords: Barium Zirconate Titanate, Solid State Reaction, Dielectric Constant, Dielectric Loss

Introduction

Due to its superior dielectric and piezoelectric properties, barium titanate (BTO), a typical ferroelectric material, is frequently employed in sensors, memory, multilayer ceramic capacitors (MLCC).¹⁻⁴ However, the potential of the room temperature environment is constrained since the material's phase transition point from the cubic phase to the tetragonal phase is approximately 120°C. The researchers can increase the BTO ceramics' potential for use at room temperature. The Ba²⁺ ion's A site and the Ti⁴⁺ ion's B site are typically swapped out in the BTO system to create the majority of the modifications. Ba_{1-x}Sr_xTiO₃ (BST) is an A-site replacement for BTO ceramics, when the Sr²⁺ ion content is 30%, the Curie temperature is almost at ambient temperature.⁵⁻⁸ BST ceramics also have a better

dielectric constant and a lower leakage current density. However, the leakage current abruptly increases by an order of magnitude and even breaks down when the external electric field of the BST ceramic approaches several hundred kilovolts per centimetre, limiting its potential for use. In comparison to BST ceramics, zirconium zirconate titanate Ba (Zr_xTi_{1-x})O₃ (BZT) ceramics have greater dielectric nonlinearity and lower dielectric loss. In contrast to Ti⁴⁺ ions, Zr⁴⁺ ions have larger ionic radii. Zirconium titanate (BZT) can be a good alternative to BST since the chemical structure is more stable when the Ti⁴⁺ ion is replaced with Zr⁴⁺ ions. Barium titanate and barium zirconate are combined to form the BZT ceramic, which can be dissolved in any ratio because they are both totally solid solutions. Additionally, the three phase transition temperatures

of BTO ceramics—90 °C, 5 °C, 120 °C—are close to one another as zirconium content increases. The three phase transition points coincide when zirconium content exceeds 15%, which is advantageous for the dielectric.⁹⁻¹¹ In order to study the use of BZT ceramics with a Zr⁴⁺ content of 5–20% in high voltage capacitors, Yan Zhang et al. produced BZT ceramics using the solid state reaction method.¹² BaZr_{0.1}Ti_{0.9}O₃ ceramics' structure, dielectric, ferroelectric properties have been reported to be impacted by ZnO doping by Aditya Jain et al.¹³ BaTi_{0.95}Zr_{0.05}O₃ ceramics were made by the hydrothermal method, Zixiong Sun et al. investigated the impact of immersion duration on grain size, dielectric, ferroelectric properties.¹⁴ Numerous papers emphasise the use of BZT ceramics, doping modification, process enhancement. There are currently few reports on the effects of various Zr/Ti components on the structural characteristics of ceramics made of lanthanum zirconate titanate. The study and practical use of BZT ceramics, however, are where this work's relevance lies.

In this study, solid-state reaction was used to examine the effects of the Zr/Ti ratio on the crystal structure, grain size, dielectric characteristics of Ba(Zr_xTi_{1-x})O₃ (x=0.15, 2.0, 2.5, 3.0) ceramics.

Experimental Procedures

Ceramics made of Ba(Zr_xTi_{1-x})O₃ (x=0.15, 2.0, 2.5, 3.0) were created using a traditional solid phase reaction preparation method. BaCO₃, TiO₂, ZrO₂ were the powder raw ingredients used to make ceramics (Alfa Aesar, 99.8%, 99.5%, Aladdin, 99.99%, respectively). The powdered raw materials were weighed in accordance with the molar ratio, introduced to an agate ball-filled nylon ball mill jar, given a suitable amount of absolute ethanol as a ball milling medium for planetary ball milling for a period of 12 hours. After ball milling, the slurry was removed, maintained for 12 hours, dried at 1150 degrees Celsius. In an agate mortar, the calcined material was crushed before being ball milled one more for 24 hours. Polyvinyl alcohol (PVA) was used as a granulation binder at 5% after drying. Ceramics made of Ba(Zr_xTi_{1-x})O₃ (x=0.15, 2.0, 2.5, 3.0) were created using a traditional solid phase reaction preparation method. BaCO₃, TiO₂, ZrO₂ were the powder raw ingredients used to make ceramics (Alfa Aesar, 99.8%, 99.5%, Aladdin, 99.99%, respectively). The powdered raw materials were weighed in accordance with the molar ratio, introduced to an agate ball-filled nylon ball mill jar, given a suitable amount of absolute ethanol as a ball milling medium for planetary ball milling for a period of 12 hours. After ball milling, the slurry was removed, maintained for 12 hours, dried at 1150 degrees Celsius. In an agate mortar, the calcined material was crushed before being ball milled one more for 24 hours. Polyvinyl alcohol (PVA) was used as a granulation binder at 5% after drying. The press used 20 MPa of pressure to press the green body, which had a

diameter of =10 mm and a thickness of d=1 mm. The final ceramic sample was created by holding at 1350°C for 4 hours after the PVA adhesive had been released by heating at 600°C for 0.5 hours. In order to ensure that the electrode made good contact with the prepared ceramic sample and minimise test error, it was double-sided polished, coated with silver paste, heated to 600°C for 0.5 hours. An X-ray diffractometer (Rigaku Ultima IV) was used to examine the crystal structure of the BZT ceramic sample, a scanning electron microscope (JSM-6390LV) was used to examine the microscopic morphology.

The press used 20 MPa of pressure to press the green body, which had a diameter of =10 mm and a thickness of d=1 mm. The final ceramic sample was created by holding at 1350°C for 4 hours after the PVA adhesive had been released by heating at 600°C for 0.5 hours. In order to ensure that the electrode made good contact with the prepared ceramic sample and minimise test error, it was double-sided polished, coated with silver paste, heated to 600°C for 0.5 hours. An X-ray diffractometer (Rigaku Ultima IV) was used to examine the crystal structure of the BZT ceramic sample, a scanning electron microscope (JSM-6390LV) was used to examine the microscopic morphology. The lattice constants a and c are calculated from the formula $c=(2d_{002})$ and

$$a = \frac{2}{\sqrt{\frac{1}{d_{100}^2} + \frac{1}{d_{110}^2}}} \quad [15].$$

The density of the ceramic is determined by the Archimedes principle. Dielectric properties were measured by an impedance analyzer (Keysight E4990A), which was completed using a liquid-free physical synthesis test system (Quantum Design, PPMS). The dielectric constant is obtained by the following formula:

$$\varepsilon = \frac{Cd}{\varepsilon_0 A} \quad (1)$$

An XRD pattern of a BZT ceramic sample is shown in Figure 1a. All of the samples have a perovskite cubic phase structure with full diffraction peaks and no second phase, proving that Zr⁴⁺ has fully substituted the B-site inside the lattice. An enlarged image of the (002) diffraction peak at 45° can be found in Fig. 1(b). The (002) peak position of the BZT-15 sample and the (002) peak position of the BZT-30 sample are both clearly visible in the figure. As the Zr content rises, the peak's position at 44.6° moves to a slight inclination. The principal cause is that the Ti⁴⁺ ion has a radius of 0.0605 nm while the Zr⁴⁺ ion has a radius of 0.072 nm. The lattice constant is slightly distorted as the Zr⁴⁺ ion takes the place of the Ti⁴⁺ ion. According to Fig. 2, the lattice constants a and c gradually rise with increasing Zr content, the ratio a/c roughly stays at 1, showing that the cubic phase structure of the BZT ceramics does not change. in line with the XRD pattern. Figure 3 shows a SEM image of a BZT ceramic with various Zr/Ti compositions. The ceramic samples in (a-d) correspond to BZT-15, BZT-

20, BZT-25, BZT-30, respectively. The SEM image makes it easy to see the ceramic sample's microstructure. The uniform grain size and distinct grain boundaries in the photograph suggest that all of the ceramic samples' crystals are generally flawless.

The average grain size in Fig. (a) is about 6 μm , there are a few small holes here and there. First, the BZT-15 sample's bigger grain size and increased likelihood of defects in the grain development process caused by grain combination and grain boundary fusion result from the sample's faster growth in the sintering temperature zone. Second, when the Zr concentration is low, the sinterability is bad and the crystal grains' surfaces develop tiny pores. The average grain distribution is more even and compact, the ceramic sample structure is denser, the average grain size is 4 μm in Figure (b), which is also favourable to the liquid phase sintering effect. According to Fig. (d), the average grain

size is only 2.5 μm when the Zr content is 30%. It is evident from comparing the SEM images of the four distinct Zr/Ti compositions in Figure 3(a-d) that the grain size steadily shrinks as the Zr concentration rises. In comparison to the Ti-O bond, the Zr-O bond has a greater bond energy (Zr-O bond: 776.1 kJ/mol vs. Ti-O bond: 672.4 kJ/mol). Ti^{4+} is replaced by Zr^{4+} in order to offer more energy as Zr^{4+} content rises. With an increase in Zr^{4+} content, BZT ceramics' ideal sintering temperature rises.

The four samples created for this study had a sintering temperature of 1300 $^{\circ}\text{C}$, therefore the grain size shrank as the Zr content rose. On the other hand, the fusing of grain borders and the annexation of small grains are the two fundamental factors that determine grain growth. As Zr concentration rises, ion mobility declines because Zr^{4+} has a higher ionic radius than Ti^{4+} , making it difficult for grain boundaries to move. The grain is smaller.¹⁶⁻¹⁷

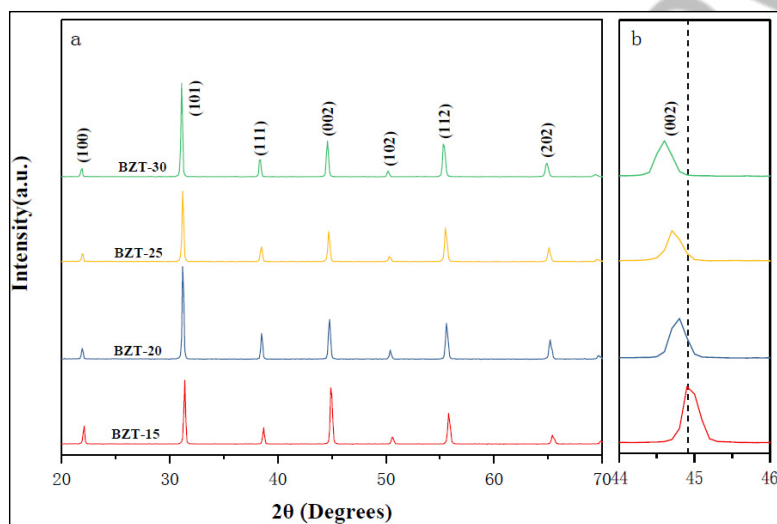


Figure 1. The XRD patterns of $\text{Ba}(\text{Zr}_x\text{Ti}_{1-x})\text{O}_3$ ceramics at different Zr/Ti ratio

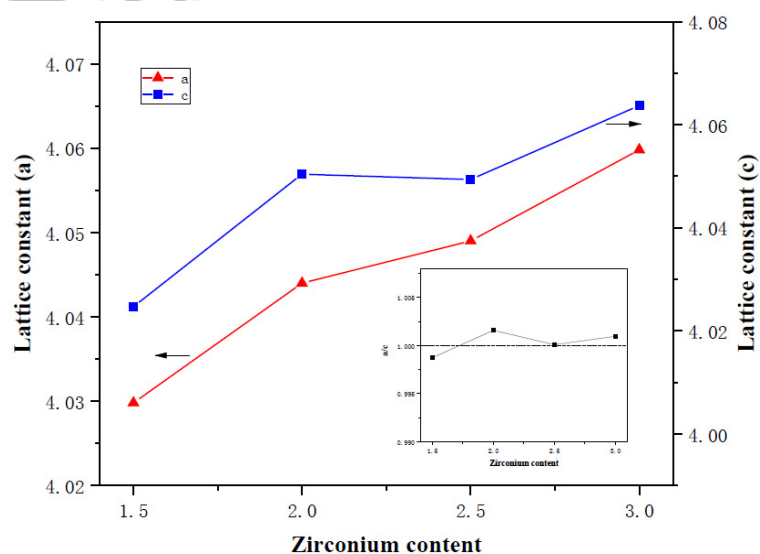


Figure 2. Lattice constant of $\text{Ba}(\text{Zr}_x\text{Ti}_{1-x})\text{O}_3$ ceramics at different Zr/Ti ratios

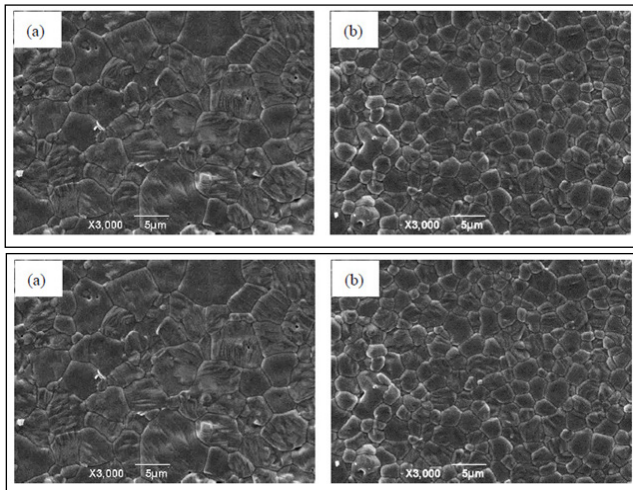


Figure 3. SEM photos of Ba(Zr_xTi_{1-x})O₃ ceramics at different Zr/Ti ratios

The density curves of BZT ceramic samples with various zirconium concentrations are shown in Figure 4. All BZT ceramic samples had densities of 97% or above. The density of the BZT-15 sample is relatively low, the density of the BZT ceramic sample rises with increasing Zr⁴⁺ ion content and falls when Zr content reaches 30%, which is consistent with the SEM image of Fig. 3 and the figure. The BZT-15 sample's high grain growth during the sintering process makes it more likely that the grains would develop flaws, which will lead to a low-density phenomena. Because grain size decreased as Zr⁴⁺ ion content increased, the BZT-30 sample's density decreased. Smaller grain sizes produce more grain boundaries per unit volume, smaller grain boundary density, more flaws, which results in a drop in density.

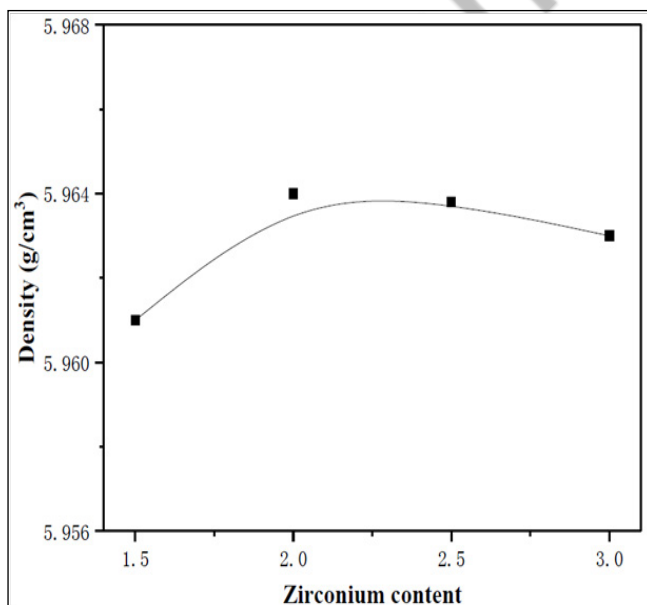


Figure 4. Density curve of Ba(Zr_xTi_{1-x})O₃ ceramics at different Zr/Ti ratios

The dielectric constant and dielectric loss of a BZT ceramic sample with various Zr/Ti compositions are plotted in Figure 5 using temperature at 1 kHz measurements. The figure makes the BZT-15 sample very obvious to view. Of all the samples, it possesses the best dielectric qualities. 11050 is the highest possible dielectric constant. There is a noticeable dielectric peak. As the Zr concentration rises and is spread out, the dielectric peak steadily rises. As the Zr content rises, as seen in Fig. 6, the dielectric constant gradually drops. On the one hand, the huge grain size of BZT-15 causes the grain size to decrease as the Zr content rises, the grain size has a significant impact on the dielectric constant. Samples with greater grain sizes exhibit improved dielectric characteristics, according to Zheng Sun et al.¹⁸ On the other hand, BZT ceramics are solid mixtures of BTO and BZO since BaZrO₃ (BZO) lacks ferroelectricity. The composition of BZO steadily changes as Zr content rises, decreasing the dielectric characteristics of BZT ceramics. On the other hand, the barium titanate ceramic has three phase transition points, which are the trigonal phase to the oblique phase, the oblique phase to the tetragonal phase, the tetragonal phase to the cubic phase. As the Zr content rises, the three phase transition points become more contiguous. The three phase transition points all coincide with a Zr concentration of 15%, the corresponding phase transition points improve the dielectric characteristics. It is easy to detect the dielectric loss with temperature curve in Figure 5. There are reports of two dielectric loss peaks T₁ and T₂, which arise at 300K and 125K, respectively.²¹ Both peaks shift towards the low temperature zone as the Zr content rises. It is also evident that the dielectric loss T₁ gradually lowers while the dielectric loss T₂ gradually rises, which may be a result of lattice distortion brought on by an increase in the Zr concentration.

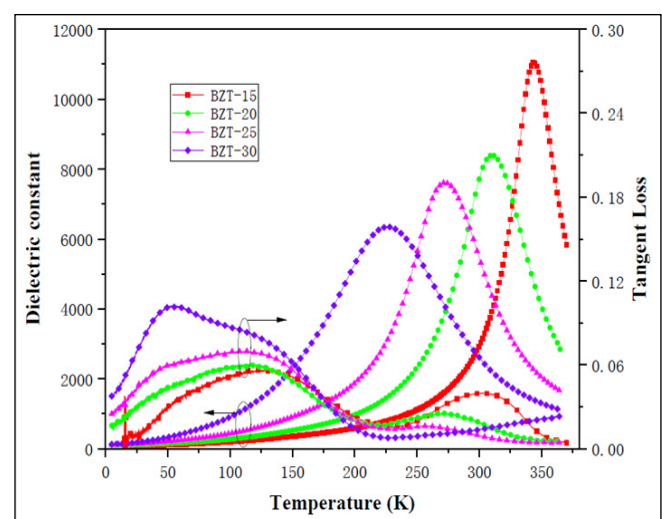


Figure 5. The dielectric constant and dielectric loss curve of Ba(Zr_xTi_{1-x})O₃ ceramics with different Zr/Ti ratios

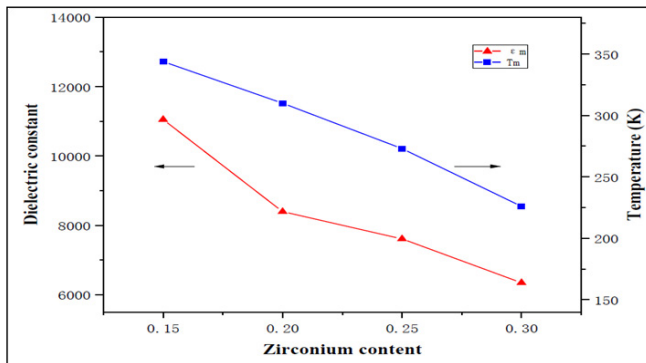


Figure 6. Maximum dielectric constant and corresponding temperature of $Ba(Zr_xTi_{1-x})O_3$ ceramics with different Zr/Ti ratio

The dielectric constant and dielectric loss for BZT ceramic samples with various Zr concentrations are plotted against frequency variation in Figure 7 at room temperature. The BZT-20 sample has the highest dielectric constant, which declines with increasing Zr content, as depicted in the figure. However, the BZT-15 sample in Figure 5 has the highest dielectric constant, in Figure 7's dielectric spectrum, the sample is just slightly higher than the BZT-30 sample. The lower polarisation of the BZT-15 sample results in a lower dielectric constant in a room-temperature environment since the Curie temperature of the sample is 344K, which is substantially higher than room temperature. BZT-20 has a Curie temperature of 310K. The BZT-20 sample has the highest dielectric constant in this curve since it was measured at room temperature. The BZT-15 and BZT-30 samples fluctuate dramatically with frequency in the low frequency portion of the dielectric loss with frequency curve, there is a significant dielectric loss. As frequency rises, the dielectric loss curve gradually becomes stable. Because interfacial polarisation, ion displacement polarisation, electron displacement polarisation make up the majority of the ceramic sample's polarisation in the low frequency range. In the high frequency area, interfacial polarisation and ion displacement polarisation play the primary roles. Ion displacement polarisation and electronic displacement polarisation play a part. Due to frequency and high dielectric loss in the low frequency zone, two samples of BZT-15 and BZT-30 were impacted, most likely because certain samples contained macro flaws, but the causes of creation varied. The BZT-15 sample might be defective due to interlayers and bubbles in the mutual annexation of the grains and the fusing of the grain borders, as well as faster and larger grain development during the sintering process. These polarisation process flaws exist. More internal energy and space charge are produced. The significant dielectric loss of BZT-15 samples in the low frequency range is mostly caused by these reasons. The key factor affecting the sample of BZT-30 at low frequencies is its tiny grain size, which results in more grain boundaries per unit volume

regardless of whether the ferroelectricity of the grain boundary is small or not. Ferroelectricity also has a high likelihood of producing macroscopic flaws at the grain boundary, which causes a high dielectric loss in the low frequency range. In accordance with the XRD pattern, the dielectric loss of the four samples gradually stabilised with increasing frequency, showing that the crystallisation is more complete and there are fewer flaws at the microscopic and structural levels.

Conclusions

Solid phase reaction was carried out at 1350°C for 4 hours to produce $Ba(Zr_xTi_{1-x})O_3$ ceramics ($X=1.5, 2.0, 2.5, 3.0$). By examining crystal structure, morphology, density, dielectric properties, it was possible to determine how the Zr/Ti ratio affected the characteristics of BZT ceramics. The findings demonstrate that the dielectric constant at 15% Zr concentration is 11050, the highest of all samples, the dielectric loss is only 0.014. The dielectric constant falls, the dielectric peak widens, the grain size shrinks, the lattice constant rises, the Curie temperature falls from 344K to 226K as Zr concentration rises. The Curie temperature, which is 310K when Zr is 20%, is the temperature that is most similar to ambient temperature.

References

1. Scott JF (2007) Applications of modern ferroelectrics J Science 315: 954-959.
2. Li Y, Moon KS, Wong CP (2005) Electronics without Lead J Science 308:1419-1420.
3. Liu W, Ren X (2009) Large piezoelectric effect in Pb-free ceramics J Phys rev lett 103: 257602.
4. Hennings D, Schnell A, Simon G (2010) Diffuse Ferroelectric Phase Transitions in $Ba(Ti_{1-y}Zr_y)O_3$ Ceramics J Journal of the American Ceramic Society 65: 539-544.
5. Mitsui T, Nakamura E, Shiozaki Y (2006) Introduction containing a detailed survey of all substances and properties of Vol. III/36C: Organic crystals, liquid crystals and polymers[M]// Organic crystals, liquid crystals and polymers. Springer Berlin Heidelberg 2006: 437-440.
6. Chen H, Yang C, Fu C, Jun Shi, Jihua Zhang, et al. (2008) Microstructure and dielectric properties of $BaZr_xTi_{1-x}O_3$ ceramics J Journal of Materials Science Materials in Electronics 19: 379-382.
7. Chen CL, Shen J, Chen S Y, Luo GP, Chu CW (2001) Epitaxial growth of dielectric $Ba_{0.6}Sr_{0.4}TiO_3$ thin film on MgO for room temperature microwave phase shifters. J Applied Physics Letters 78: 652-654.
8. Acikel B, Taylor TR, Hansen PJ, Speck JS, York RA (2002) A new high performance phase shifter using $Ba_{x/Sr_{1-x}}TiO_3$ thin films J IEEE Microwave & Wireless Components Letters 12: 237-239.

9. Moura F, Simões AZ, Stojanovic BD, Maria Aparecida Zaghete, Elson Longo, et al. (2008) Dielectric and ferroelectric characteristics of barium zirconate titanate ceramics prepared from mixed oxide method J Journal of Alloys & Compounds 462: 129-134.
10. Liang D, Zhu X, Zhu J, JianguoZhu, Dingquan Xiao (2014) Effects of CuO addition on the structure and electrical properties of low temperature sintered Ba(Zr,Ti)O₃ lead-free piezoelectricceramics. J Ceramics International 40: 2585-2592.
11. Xu Y, Zhang K, Fu L, Ting Tong, Le Cao, et al. (2019) Effect of MgO addition on sintering temperature, crystal structure, dielectric and ferroelectric properties of lead-free BZT ceramics. J Mater Sci: Mater Electron 30: 7582-7589.
12. Zhang Y, Li Y, Zhu H, Zhenxiao Fu, Qitu Zhang (2016) Influence of Zr/Ti ratio on the dielectric properties of BaZr_xTi_{1-x}O₃, ceramics for high-voltage capacitor applications. Journal of Materials Science: Materials in Electronics 27: 9572-9576.
13. Jain A, Panwar AK, Jha AK (2016) Effect of ZnO doping on structural, dielectric, ferroelectric and piezoelectric properties of BaZr_{0.1}Ti_{0.9}O₃ ceramics. Ceramics International 43: 1948-1955.
14. Sun Z, Pu Y, Dong Z, Yao Hu, Xiaoyan Liu, et al. (2014) The effects of soaking time on the grain growth, dielectric and ferroelectric properties of BaTi_{0.95}Zr_{0.05}O₃, ceramics prepared by microwave sintering. Vacuum 101: 228-232.
16. Wang DY, Wang Y, Zhou XY, Chan HLW, Choy CL (2005) Enhanced in-plane ferroelectricity in Ba_{0.7}Sr_{0.3}TiO₃ thin films grown on MgO (001) single-crystal substrate. Applied Physics Letters 86: 416.
17. Ciomaga CE, Buscaglia MT, Viviani M, Buscaglia V, Mitoseriu L, et al. (2006) Preparation and dielectric properties of BaZr_{0.1}Ti_{0.9}O₃ ceramics with different grain sizes. Phase Transitions 79: 389-397.
18. Lee SG, Kang DS (2003) Dielectric properties of ZrO₂-doped (Ba,Sr,Ca)TiO₃ ceramics for tunable microwave device applications. Materials Letters 57: 0-1634.
19. Sun Z, Li L, Zheng H, Shihui Yu, Dan Xu (2015) Effects of sintering temperature on the microstructure and dielectric properties of BaZr_{0.2}Ti_{0.8}O₃, ceramics. Ceramics International 41: 12158-12163.
20. Reddy SB, Rao MSR, Rao KP (2007) Observation of high permittivity in Ho substituted BaZr_{0.1}Ti_{0.9}O₃ ceramics. Applied Physics Letters 91: 91.
21. Pisitpipathsin N, Kantha P, Pengpat K, Gobwute Rujijanagul (2013) Influence of Ca substitution on microstructure and electrical properties of Ba(Zr,Ti)O₃, ceramics. Ceramics International 39: S35-S39.
22. Tang XG, Chew KH, Chan HLW (2004) Diffuse phase transition and dielectric tunability of Ba(Zr_yTi_{1-y})O₃ relaxor ferroelectric ceramics. Acta Materialia 52: 5177-5183.
23. Tang XG, Chew KH, Chan HLW (2004) Diffuse phase